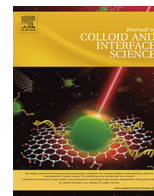




Contents lists available at ScienceDirect

Journal of Colloid and Interface Science

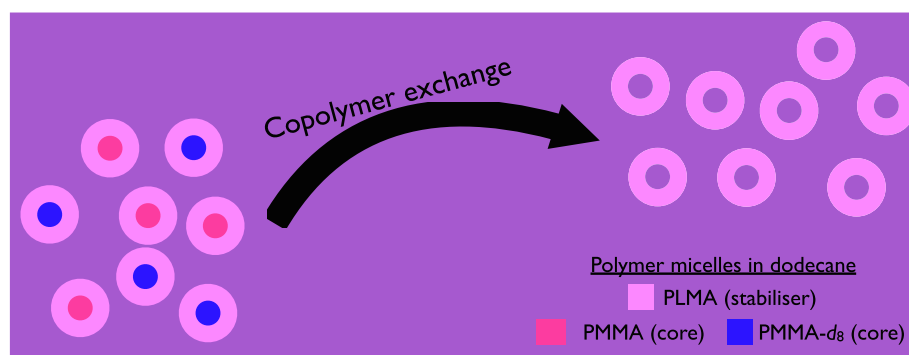
journal homepage: www.elsevier.com/locate/jcis

Short Communication

Molecular exchange in spherical diblock copolymer colloids synthesised by polymerisation-induced self-assembly

Gregory N. Smith^{a,b,*}, Isabelle Grillo^{c,1}, James E. Hallett^{d,2}^a Department of Chemistry, University of Sheffield, Brook Hill, Sheffield, South Yorkshire S3 7HF, United Kingdom^b Niels Bohr Institute, University of Copenhagen, H. C. Ørsted Institute, Universitetsparken 5, 2100 Copenhagen Ø, Denmark^c Institut Laue–Langevin, 71 Avenue des Martyrs, 38042 Grenoble Cedex 9, France^d H. H. Wills Physics Laboratory, University of Bristol, Tyndall Avenue, Bristol, BS8 1TL, United Kingdom

GRAPHICAL ABSTRACT



ARTICLE INFO

Article history:

Received 6 April 2020

Revised 4 June 2020

Accepted 5 June 2020

Available online 15 June 2020

Keywords:

Colloids

Small-angle neutron scattering

Molecular exchange

Polymer micelles

Polymerisation-induced self-assembly

Hypothesis: To study molecular exchange between colloids requires the preparation of suitably labelled species. Deuterium isotopic labelling has been used to prepare two chemically identical yet isotopically distinguishable poly(lauryl methacrylate)–poly(methyl methacrylate) (PLMA–PMMA) diblock copolymer colloids by polymerisation-induced self-assembly (PISA) directly in an alkane solvent. Molecular exchange should be detectable by performing small-angle neutron scattering (SANS) measurements on the dispersions.

Experiments: SANS measurements were performed on fully hydrogenous PLMA₃₉–PMMA₅₇ and deuterated core PLMA₃₉–P(MMA-*d*₈)₅₇ colloids. They were mixed in equal amounts and heated to determine if molecular exchange occurred. PISA syntheses are often thermally initiated, and diblock copolymers self-assemble at elevated temperature, making this an important parameter to study. Experimental data for the mixture were compared to predicted curves for exchanged and non-exchanged colloids.

Findings: The scattering of a mixture of fully hydrogenous and deuterated core copolymers does not disappear upon molecular exchange, due to the remaining contrast between the stabiliser and the core and solvent even after the cores fully exchange. By simultaneously fitting the SANS data from dispersions before mixing and using these parameters to constrain fitting the SANS data of mixtures, the molecular exchange between diblock copolymer micelles upon heating is clearly observed.

© 2020 The Author(s). Published by Elsevier Inc. This is an open access article under the CC BY license (<http://creativecommons.org/licenses/by/4.0/>).

* Corresponding author at: Niels Bohr Institute, University of Copenhagen, H. C. Ørsted Institute, Universitetsparken 5, 2100 Copenhagen Ø, Denmark.

E-mail address: gregory.smith@nbi.ku.dk (G.N. Smith).

¹ Deceased: 5 August 2019.

² Current address: Physical & Theoretical Chemistry Laboratory, Oxford University, South Parks Road, Oxford OX1 3QZ, United Kingdom.

1. Introduction

Significant insight has been gained into the self-assembly of block copolymers [1–10] through the use of molecular exchange, a long-studied topic in colloid science [11–15]. To study the exchange of molecules between environments requires some form of labelling to identify the species uniquely while maintaining their chemical identity. Deuterium isotopic labelling with small-angle neutron scattering and fluorescence labelling with lifetime spectroscopy are two previously employed methods [16–24].

Self-assembled block copolymers are very interesting and important materials, both in terms of their growing potential for application and in the variety of morphologies that can be accessed [25]. Early examples of diblock polymer nano-objects were synthesised using post-polymerisation solvent exchange to reduce the solvent quality for one block [26–28]. Recently, polymerisation-induced self-assembly (PISA) has emerged as a convenient and advantageous way to produce polymer micelles rationally, at high concentrations, and directly in a solvent of interest [29]. It is very versatile and has been demonstrated in water [30], alcohols [31,32], aliphatic solvents [31,32], supercritical carbon dioxide [33], and ionic liquids [34]. The ability to synthesise particles during the polymerisation reaction is a particular advantage of the PISA process. While many of the previous reports using deuterium isotopic labelling to study the exchange between polymer micelles have revealed very interesting aspects of the process, they rely on post-polymerisation methods to prepare colloids [1,3,6,21,22]. These numerous examples of the application of small-angle neutron scattering (SANS) to the study of the self-assembly and molecular exchange of block copolymers demonstrate the value of this technique [1–10,21,22]. The application of neutron scattering to colloids synthesised by PISA, which produces block copolymers that are similar to post-polymerisation methods but offers the particular advantages discussed above, is more limited [35–39]. As particles synthesised by PISA are prepared directly during the polymerisation reaction, molecular exchange during the particle formation process could be significant. Gaining a better understanding of this exchange process for particles synthesised by PISA is what we set out to understand.

SANS has been used to study whether or not exchange occurs between spherical diblock copolymer micelle colloids. The colloids of interest are poly(lauryl methacrylate)–poly(methyl methacrylate) (PLMA–PMMA) diblock copolymers synthesised by PISA with either hydrogenous PMMA cores (PLMA–PMMA) or deuterated PMMA cores (PLMA–PMMA- d_8), shown in Fig. 1. These colloids were then dispersed, either on their own or as mixtures in PMMA/PMMA- d_8 core-average dodecane solvent. The PLMA block is hydrogenous in both cases. The large molecular volume of the LMA monomer compared to the MMA monomer means that the PLMA block significantly scatters in both cases. As these particles, along with many other spheres prepared by PISA, are synthesised using thermally-initiated radical polymerisation [40], the molecular exchange is studied both before mixing and after mixing with heating to determine the degree to which molecular exchange occurs during PISA reactions. The kinetics of molecular exchange in PLMA–PMMA diblock copolymer micelles synthesised by PISA was recently studied by time-resolved SANS, which showed that the SANS data change with time and eventually reach a steady state. However, it was not possible to fit the SANS data to an appropriate model, and this limited the ability to monitor the structure of the micelles throughout the exchange process [41]. The ability to model the SANS data for these PLMA–PMMA micelles should make it possible to determine to what extent the exchange process occurs. Furthermore, it would also allow the rate of reaction to be monitored via the change in contrast between the micelle and

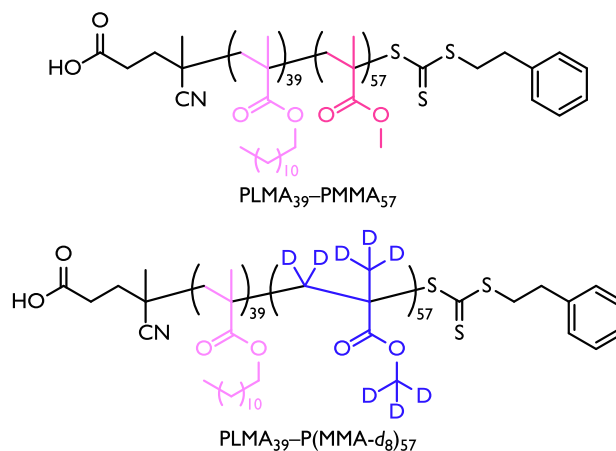


Fig. 1. The structure of the two poly(lauryl methacrylate)–poly(methyl methacrylate) diblock copolymers used to form spherical nanoparticles. One is fully hydrogenous (PLMA₃₉–PMMA₅₇, top), and the other is partially deuterated in the core-forming block (PLMA₃₉–P(MMA- d_8)₅₇, bottom), resulting in a partially deuterated colloid with an isotopically-labelled core.

solvent, rather than through the scattering intensity alone. These advantages are what we sought to achieve by finding an approach to modelling the SANS data.

In this study, we obtain new and independent SANS data before and after heating the polymer micelles, which is also before and after the exchange process would have occurred, and are able to describe the data using an appropriate model. By successfully fitting SANS data in these limits, we are able to determine how completely the cores of these polymer micelles (synthesised by PISA) exchange.

2. Materials and methods

2.1. Isotopically-labelled PLMA₃₉–PMMA₅₇ diblock copolymer micelles

The poly(lauryl methacrylate) (PLMA) macromolecular chain-transfer agent and poly(lauryl methacrylate)–poly(methyl methacrylate) (PLMA–PMMA) diblock copolymers were synthesised [41] using the same general procedure previously used to prepare poly(lauryl methacrylate)–poly(benzyl methacrylate) diblock copolymers [42–45]. The only difference is that the benzyl methacrylate monomer was exchanged for either methyl methacrylate (hydrogenous) or methyl methacrylate- d_8 (deuterated) monomers, to give the desired isotopic labelling. The diblock copolymers were synthesised in mineral oil, and then diluted into PMMA/PMMA- d_8 core-average dodecane solvent to give a concentration of ~ 1 vol.%. The degree of polymerisation of the PLMA stabiliser used as macromolecular chain-transfer agent was 39 and of both the PMMA and PMMA- d_8 cores was 57. Mineral oil has a viscosity similar to a long-chain aliphatic hydrocarbon [46] and is known to result in nanoparticle morphologies via PISA that are very similar to dodecane [44]. Therefore, as it is the minority component of the hydrogenous solvent, it is assumed to have the same density and neutron scattering length density as hydrogenous dodecane. An equivalent amount of mineral oil was added to the background solvent for subtraction, and the amount of hydrogenous dodecane for contrast matching was adjusted by the presence of this hydrogenous alkane (mineral oil) solvent. The neutron scattering length densities of the polymers and solvents (SLD, ρ_n) were calculated using the mass densities (ρ_m) from literature and the neutron scattering lengths [47] and are shown in Table S1 in the Supporting Material. The SLD of mixtures were calculated as a vol-

ume fraction (ϕ) weighted sum of the individual components ($\sum_i \phi_i \rho_{n,i}$).

2.2. Small-angle neutron scattering

Small-angle neutron scattering (SANS) measurements were performed on the instrument D33 at the Institut Laue–Langevin (ILL; Grenoble, France) [48]. The intensity was calculated as a function of Q , the magnitude of the momentum transfer vector, which depends on half the scattering angle (θ) and the neutron wavelength (λ) [49].

$$Q = \frac{4\pi \sin \theta}{\lambda} \quad (1)$$

Two configurations were used with different sample-detector distances (L_D) and collimation distances (L_C), with the same wavelength $\lambda = 6 \text{ \AA}$ (configuration 1: $L_D = 12 \text{ m}$, $L_C = 12.8 \text{ m}$, $\lambda = 6 \text{ \AA}$; configuration 2: $L_D = 2 \text{ m}$, $L_C = 5.3 \text{ m}$, $\lambda = 6 \text{ \AA}$). This gave an accessible Q -range of $0.0037 < Q < 0.46 \text{ \AA}^{-1}$. The beam size was 7 mm by 10 mm . SANS measurements were performed on pure dispersions of PLMA₃₉–PMMA₅₇ and PLMA₃₉–P(MMA-*d*₈)₅₇, and on a 1:1 volume ratio mixture of the two after heating to $150 \text{ }^\circ\text{C}$ for 1 h . A 1 mm thick sample of liquid water (H_2O) was measured to correct the detector intensity. Raw data were integrated, normalised with respect to transmission, and stitched together using instrument-specific software, LAMP. Data were modelled as explained in the text using the SasView 5.0.2 package [50]. The calculated fits were smeared by dQ calculated during reduction in LAMP.

3. Results and discussion

Dispersions of the PLMA₃₉–PMMA₅₇ and PLMA₃₉–P(MMA-*d*₈)₅₇ polymer micelles have dramatically different SANS data, shown in Fig. 2. The difference between the fully hydrogenous and deuterated core polymer micelles is in contrast to previous experiments on fully-deuterated diblock copolymer micelles [22], as the diblock copolymers used in this study are only core-deuterated. While fully-deuterated diblock copolymers would be preferable, synthesising deuterated poly(lauryl methacrylate) has proved to be extremely challenging [51].

The SANS data can be fit using the model of Pedersen and Gerstenberg [52,53] for spherical polymer micelles (spherical polymer core with Gaussian polymer chains attached to the surface), as implemented in SasView [54]. The form factor ($P(Q)$) is given as the sum of two self-terms (P_s for the spherical cores and P_c for the Gaussian chains on the surface) and two cross-terms (S_{sc} between the cores and the Gaussian chains and S_{cc} between the chains on the surface themselves). In this expression, N is the aggregation number, and β_s and β_c are the total excess scattering lengths of blocks in the core (spherical cores) and the shell (chains), respectively. These are given by $\beta_i = V_i(\rho_i - \rho_m)$, where V_i is the volume of a block, ρ_i is the SLD of a block, and ρ_m is the SLD of the medium.

$$P(Q) = N^2 \beta_s^2 P_s(Q) + N \beta_c^2 P_c(Q) + 2N^2 \beta_s \beta_c S_{sc}(Q) + N(N-1) \beta_c^2 S_{cc}(Q) \quad (2)$$

The sphere self-term is the well-known spherical form factor ($P_s(Q)$) for a sphere with radius r [55,56]. In the SasView implementation [54], there is no size distribution. Furthermore, the radius r is used to determine the value of N from the volume of the core and V_s . This is a separate fitting parameter, but we have fixed it and iterated fitting the radius until the value of N converges.

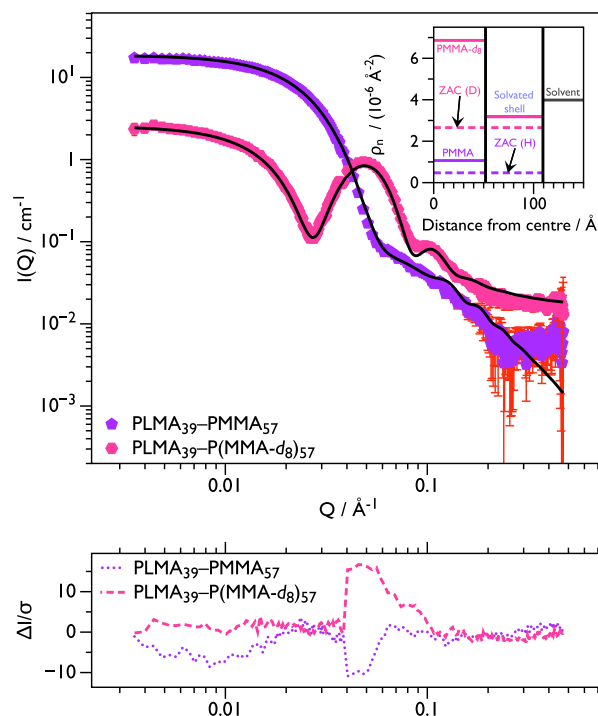


Fig. 2. SANS data for dilute dispersions of PLMA₃₉–PMMA₅₇ and PLMA₃₉–P(MMA-*d*₈)₅₇ in PMMA/PMMA-*d*₈ core-average dodecane. The experimental and fit scattering curves ($I(Q)$, top) and the error-weighted residual difference plots ($\Delta I/\sigma$, bottom) are both shown as a function of Q . Although chemically identical, the distinct isotopic composition results in very different scattering curves. This is due to the composition of the particles, which can be seen in the scattering length density (SLD, ρ_n) profiles of the particles as a function of distance from the particle centres. The SLDs of the cores are calculated from the homopolymer densities, the SLD of the solvated shell is the volume fraction weighted SLD of the solvent and the chains in the shell, and the SLD of the solvent is the average of the two cores. The zero-average contrast (ZAC) SLDs for the two block copolymers (denoted D and H) are also shown. The values for the two polymers are different from the core polymer to varying degrees, due to the significant volume of the PLMA stabiliser.

$$P_s(Q) = \left[\frac{3[\sin(Qr) - Qr \cos(Qr)]}{(Qr)^3} \right]^2 \quad (3)$$

The Gaussian chain self-term for chains in the corona is given by the Debye function ($P_c(Q)$) for a polymer chain with radius of gyration R_g [57].

$$P_c(Q) = \frac{2[\exp(-Q^2 R_g^2) - 1 + Q^2 R_g^2]}{(Q R_g^2)^2} \quad (4)$$

The sphere-chain cross-term ($S_{sc}(Q)$) and the chain-chain cross-term ($S_{cc}(Q)$) are available elsewhere [53] and are not reproduced here.

The fit data and corresponding scattering length density profiles are shown in Fig. 2, and the best fit values are given in Table S2 in the Supporting Material. The error-weighted residual difference plot [58] ($\Delta I/\sigma = (I_{\text{exp}} - I_{\text{fit}})/\sigma$) where I_{exp} and I_{fit} are the experimental and fit scattering intensities, respectively, and σ is the uncertainty of the experimental scattering intensity, is shown alongside these for every value of Q and both sets of data over the entire Q range. This enables the quality of the fits to be compared between the two polymer micelles. It is important to emphasise that the two curves are fit simultaneously, with parameters (aside from the core SLD, Table S1 in the Supporting Material) constrained to fit to the same values. The SLD (ρ_n) profile as a distance

from the particle centre is also shown as an inset in Fig. 2. This graphically shows that the difference between the two polymer micelles is in the core only and that the solvated shell and solvent are the same. The zero-average contrast (ZAC) SLDs, which are the volume fraction weighted SLD of the two blocks, are also shown. Because the polymers both have a large volume and hydrogenous PLMA stabiliser block, the ZAC SLD differs significantly from the PMMA/PMMA- d_8 core-average SLD of the solvent as well as from the SLD of the core polymer. That both sets of data are fit so satisfactorily gives confidence in these fit values.

The initial block volumes were calculated from the mass densities of the polymers, taken from the literature. (These are shown in the Supporting Material, Table S1.) The R_g of the PLMA₃₉ stabiliser was calculated from the contour length of the polymer (the product of the degree of polymerisation and the length of two carbon-carbon bonds in an all *trans* configuration, 2.54 Å, which is calculated from the bond length of two C-C bonds in similar sp^3 carbons and the C-C-C bond angle of gas phase propane [59–61]) and the Kuhn length of PLMA (30 Å, taken from the literature [62,63]). Assuming that the polymers are Gaussian coils, the R_g can be calculated using Eq. 5 from the contour length (L) and the Kuhn length (b), where $N_b \equiv L/b$ is the number of Kuhn segments [64].

$$R_g = \sqrt{\frac{L/b}{g}} \cdot b \equiv \sqrt{\frac{N_b}{6}} \cdot b \quad (5)$$

Using these parameters to preliminarily calculate the scattering curves, the data cannot be successfully modelled. In order to obtain the best fit to these data, the volume of the PLMA chains in the corona (V_c) must be varied. No other parameter describing the chains has sufficient impact on the scattering data. This has not been required for SAXS data of PLMA-stabilised polymer micelles [43], but this is likely because the H/D isotopic-contrast in SANS results in a greater sensitivity for the scattering between this polymer and the dodecane solvent [65,66], which have very similar electron densities. While the exact origin of this is not clear, we envision two possible possibilities. Either the mass density of this specific PLMA polymer differs from the literature value (due to its molar mass), or the degree of polymerisation is different to that determined from NMR (due to experimental uncertainty of those measurements). For even well-defined polymers with low mass dispersities (\mathcal{D}_M), the distribution of molecular volumes are broad. Using Harrison's method to calculate standard deviations from dispersities [67], the molecular volume and the distribution for this PLMA₃₉ polymer ($\mathcal{D}_M = 1.13$ [41]) is $17700 \pm 6400 \text{ Å}^3$. The model used to fit the SANS data assumes a single molecular volume, and the fit molecular volume is within this range. As good fits to the data are obtained only after some modification to the anticipated inputs (Fig. 2), it is clear that fitting this parameter is necessary.

Having determined that the structure of the polymer micelles can be determined from neutron scattering data, the impact of molecular exchange on the SANS data of mixtures of the two in PMMA/PMMA- d_8 core-average dodecane can be assessed. Using the fit parameters from the individual polymer micelles (shown in Fig. 2), scattering curves can be predicted for a mixture of the two dispersions that maintain the same number concentration but have different core SLDs. The extremes of no molecular exchange (core SLDs remain the same but the number concentration of each is halved) and complete molecular exchange (core SLD is the average of PMMA and PMMA- d_8 and the number concentration is fixed) are shown alongside the data in Fig. 3. It should clearly be possible to distinguish these two cases from experimental SANS data.

Unlike in some previous studies [3,4,6,9], the scattering intensity does not reduce to 0 at complete exchange. This is because the

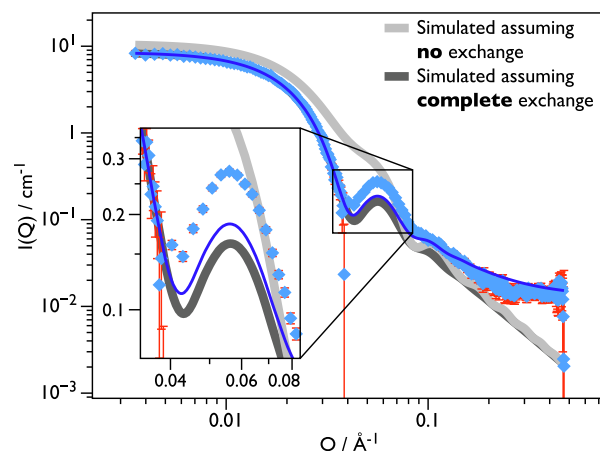


Fig. 3. SANS data for mixtures of PLMA₃₉-PMMA₅₇ and PLMA₃₉-P(MMA- d_8)₅₇ heated together and diluted in PMMA/PMMA- d_8 core-average dodecane. The data (blue diamonds) agree much better with the simulated scattering assuming complete exchange (dark grey) than the simulated scattering assuming no exchange (light grey). These data show clearly that molecular exchange occurs for these diblock copolymer micelles synthesised by PISA when heated together. (For interpretation of the references to colour in this figure legend, the reader is referred to the web version of this article.)

PLMA₃₉-P(MMA- d_8)₅₇ diblock copolymers are partially deuterated with only a deuterated core, not fully deuterated, and because the PLMA₃₉ block has a significant volume in proportion to the PMMA₅₇ and P(MMA- d_8)₅₇ blocks. This can be seen by considering how different the ZAC SLDs of the two block copolymers are from either the PMMA or PMMA- d_8 cores or the PMMA/PMMA- d_8 core-average solvent, shown in Fig. 2. The ZAC SLD of a block copolymer with the average volume and SLD of PMMA and PMMA- d_8 is $1.56 \times 10^{-6} \text{ Å}^{-2}$ (compared to $0.47 \times 10^{-6} \text{ Å}^{-2}$ for PLMA₃₉-PMMA₅₇ or $2.65 \times 10^{-6} \text{ Å}^{-2}$ for PLMA₃₉-P(MMA- d_8)₅₇), which is also not equivalent to the SLD of the PMMA/PMMA- d_8 core-average solvent ($3.96 \times 10^{-6} \text{ Å}^{-2}$). In this case, even when the mixed core is fully contrast-matched to the solvent, the PLMA stabiliser still has contrast with the solvent. Despite the SANS intensity not dropping to 0, the two situations (no exchange and complete exchange) are clearly different and should be distinguishable experimentally.

Now with an expectation of what to look for, the scattering of the mixtures of PLMA₃₉-PMMA₅₇ and PLMA₃₉-P(MMA- d_8)₅₇ polymer micelles can be assessed. The SANS data are shown in Fig. 3. Qualitatively, the scattering from the heated sample is much more similar to that predicted for complete molecular exchange than no molecular exchange. To confirm this, the data were fit to determine the exact composition of the particles. The core SLD is the only parameter that has been varied, and a good fit to the data can be obtained with this highly constrained model. The best fit SLD ($(4.041 \pm 0.003) \times 10^{-6} \text{ Å}^{-2}$) is essentially identical to that predicted by averaging those of PMMA and PMMA- d_8 ($3.958 \times 10^{-6} \text{ Å}^{-2}$). The data and the fit differ most in the region of the local maximum at $Q \approx 0.06 \text{ Å}^{-1}$, but as the $Q \rightarrow 0$ scattering intensity agrees well, this suggests that this is due to a local increase in scattering contrast. The real space equivalent magnitude of Q at this peak ($d = (2\pi)/Q$ from Bragg's Law [49]) is 104 Å , which is precisely the diameter of the core of the particles. At the local level, the cores consist of a mixture of hydrogenous and deuterated polymer chains. Using the random phase approximation (RPA) [68] and the known properties of the two polymer chains, we estimate the amount of additional scattering that could be expected from this heterogeneous core [69] to be $\sim 0.025 \text{ cm}^{-1}$. The inputs to this calculation and the predicted scattering curve are shown in Table S4 and Figure S1 in the Supporting Material.

This contribution alone is insufficient to obtain complete agreement between the data and the model, so it has not been incorporated into our fitting routine, but the fact that it is of the correct order of magnitude shows that local heterogeneities can have important consequences for SANS data of such polymer micelles.

Furthermore, SANS data for a mixture of PLMA₃₉–PMMA₅₇ and PLMA₃₉–P(MMA-*d*₈)₅₇ heated *before* combining, then diluted in PMMA/PMMA-*d*₈ core-average dodecane were measured and are shown in Figure S2 in the Supporting Material. The data are very well fit with no parameters for the two polymers (Table S5 in the Supporting Material) being varied; only the scale factors for the two populations and the background were varied. The glass transition temperature of PMMA is much greater than room temperature [70], so no exchange would be expected for this dispersion. These data show clearly that this is the case.

In summary, these measurements show that complete molecular exchange occurs for polymer micelles that are synthesised by PISA. The polymer micelles in this study were heated again after synthesis, but these measurements show that the diblock copolymer chains are sufficiently mobile to exchange upon reheating. This would suggest that exchange also occurs during synthesis, particularly for thermally-initiated radical reactions.

4. Conclusions

By using isotopically-labelled diblock copolymers and small-angle neutron scattering, we have shown that diblock copolymer micelles synthesised by PISA undergo molecular exchange. Polymer spheres prepared using this method are generated directly during the reaction, and therefore, exchange during the preparation of the particles may be particularly significant compared to polymer micelles prepared using a post-polymerisation method [3,4,6,9]. For particles synthesised by thermally-initiated PISA, this preparation at elevated temperature could increase the possibility of molecular exchange. This was demonstrated previously by recent time-resolved SANS experiments, which monitored the scattering invariant as a function of time to infer molecular exchange [41]. That analysis showed that a mixture of fully hydrogenous and deuterated core polymer micelles reached a steady state during heating. Here, we focussed on producing and studying polymer micelles at the time extremes (before exchange and after heating and presumptive exchange) and showed by successfully modelling the SANS data that the core of the micelles had exchanged after heating.

This molecular exchange merits further consideration as this can provide valuable information about the reactions used to synthesise copolymer nanoparticles by PISA, in particular, along with the molecules that produce them. Many examples of successful PISA formulations use thermally-induced radical initiation, and the results of this study suggest that they will likely be experiencing molecular exchange throughout the synthesis reactions. Recently, examples of photo-initiated PISA have been reported in the literature [71–73,40,74], and these reactions are, presumably, less likely to undergo molecular exchange during their synthesis. This may have consequences on the nanoparticles that can be produced. Whatever the exact system, however, this demonstration that SANS and isotopically-labelled diblock copolymers synthesised by PISA can reveal molecular exchange in such nanoparticles suggests variables to study that will hopefully provide useful insight into their mechanism of self-assembly.

CRedit authorship contribution statement

Gregory N. Smith: Conceptualization, Investigation, Writing - original draft, Project administration. **Isabelle Grillo:** Methodology,

Investigation, Validation, Writing - review & editing. **James E. Hallett:** Investigation, Writing - review & editing.

Declaration of Competing Interest

The authors declare that they have no known competing financial interests or personal relationships that could have appeared to influence the work reported in this paper.

Acknowledgements

The authors acknowledge Professor S. P. Armes (University of Sheffield, UK) and Dr. E.J. Cornell (previously University of Sheffield, UK; currently Tongji University, China) for producing the copolymer nanoparticles in a project funded by Lubrizol. GNS acknowledges support from Professor S.P. Armes (University of Sheffield, UK) while in his group and funding from the ERC *via* a five-year Advanced Investigator grant (PISA 320372) and EPSRC (EP/J007846). JEH acknowledges Professor C. P. Royall (University of Bristol, UK) for support and funding from the ERC *via* the NANOPRS consolidator grant, project 617266 while working in his group. This work benefited from the use of the SasView application, originally developed under NSF award DMR-0520547. SasView contains code developed with funding from the European Union's Horizon 2020 research and innovation programme under the SINE2020 project, grant agreement No 654000. In particular, Dr. S. King (ISIS Facility) is acknowledged for valuable discussions regarding the RPA in SasView and for implementing it properly in SasView 5. The Institut Laue-Langevin (experiment 9-12-478) is acknowledged for allocation of beamtime (Gregory N. Smith; EASTOE Julian; GRILLO Isabelle; HALLETT James; Jocelyn Peach and PEGG Jonathan. (2016). Surfactant-induced charging of polydimethylsiloxane-poly(methyl methacrylate) latexes in non-polar solvents. Institut Laue-Langevin (ILL) doi:10.5291/ILL-DATA.9-12-478) [75]. The authors acknowledge the UK Science and Technology Facilities Council for providing funding for travel and consumables. The open access fee was covered by FILL2030, a European Union project within the European Commission's Horizon 2020 Research and Innovation programme under grant agreement N°731096.

Appendix A. Supplementary data

Supplementary data associated with this article can be found, in the online version, at <https://doi.org/10.1016/j.jcis.2020.06.022>.

References

- [1] R. Lund, L. Willner, J. Stellbrink, P. Lindner, D. Richter, Logarithmic chain-exchange kinetics of diblock copolymer micelles, *Phys. Rev. Lett.* 96 (6) (2006), <https://doi.org/10.1103/PhysRevLett.96.068302> 068302.
- [2] R. Lund, L. Willner, D. Richter, H. Iatrou, N. Hadjichristidis, P. Lindner, Unraveling the equilibrium chain exchange kinetics of polymeric micelles using small-angle neutron scattering – architectural and topological effects, *J. Appl. Cryst.* 40 (s1) (2007) s327–s331, <https://doi.org/10.1107/S0021889807005201>.
- [3] S.-H. Choi, T.P. Lodge, F.S. Bates, Mechanism of molecular exchange in diblock copolymer micelles: Hypersensitivity to core chain length, *Phys. Rev. Lett.* 104 (2010), <https://doi.org/10.1103/PhysRevLett.104.047802> 047802.
- [4] S.-H. Choi, F.S. Bates, T.P. Lodge, Molecular exchange in ordered diblock copolymer micelles, *Macromolecules* 44 (9) (2011) 3594–3604, <https://doi.org/10.1021/ma102788v>.
- [5] R. Lund, L. Willner, J. Stellbrink, P. Lindner, D. Richter, Erratum: Logarithmic chain-exchange kinetics of diblock copolymer micelles [Phys. Rev. Lett. 96, 068302 (2006)], *Phys. Rev. Lett.* 104 (4) (2010), <https://doi.org/10.1103/PhysRevLett.104.049902> 049902.
- [6] R. Lund, L. Willner, V. Pipich, I. Grillo, P. Lindner, J. Colmenero, D. Richter, Equilibrium chain exchange kinetics of diblock copolymer micelles: Effect of morphology, *Macromolecules* 44 (15) (2011) 6145–6154, <https://doi.org/10.1021/ma200532r>.

- [7] J. Lu, S. Choi, F.S. Bates, T.P. Lodge, Molecular exchange in diblock copolymer micelles: Bimodal distribution in core-block molecular weights, *ACS Macro Lett.* 1 (8) (2012) 982–985, <https://doi.org/10.1021/mz300285x>.
- [8] T. Zinn, L. Willner, R. Lund, V. Pipich, D. Richter, Equilibrium exchange kinetics in n-alkyl-PEO polymeric micelles: single exponential relaxation and chain length dependence, *Soft Matter* 8 (2012) 623–626, <https://doi.org/10.1039/C1SM06809A>.
- [9] J. Lu, F.S. Bates, T.P. Lodge, Chain exchange in binary copolymer micelles at equilibrium: confirmation of the independent chain hypothesis, *ACS Macro Lett.* 2 (5) (2013) 451–455, <https://doi.org/10.1021/mz400167x>.
- [10] T. Zinn, L. Willner, V. Pipich, D. Richter, R. Lund, Effect of core crystallization and conformational entropy on the molecular exchange kinetics of polymeric micelles, *ACS Macro Lett.* 4 (6) (2015) 651–655, <https://doi.org/10.1021/acsmacrolett.5b00197>.
- [11] S. Yiv, R. Zana, Fast exchange of alcohol molecules between micelles and surrounding solution in aqueous micellar solutions of ionic surfactants, *J. Colloid Interface Sci.* 65 (2) (1978) 286–290, [https://doi.org/10.1016/0021-9797\(78\)90159-5](https://doi.org/10.1016/0021-9797(78)90159-5).
- [12] J. Eastoe, B. Warne, Nanoparticle and polymer synthesis in microemulsions, *Curr. Opin. Colloid Interface Sci.* 1 (6) (1996) 800–805, [https://doi.org/10.1016/S1359-0294\(96\)80084-7](https://doi.org/10.1016/S1359-0294(96)80084-7).
- [13] Y. Rharbi, M.A. Winnik, Solute exchange between surfactant micelles by micelle fragmentation and fusion, *Adv. Colloid Interface Sci.* 89–90 (2001) 25–46, [https://doi.org/10.1016/S0001-8686\(00\)00054-3](https://doi.org/10.1016/S0001-8686(00)00054-3).
- [14] A. Evilevitch, J. Rescic, B. Jönsson, U. Olsson, Computer simulation of molecular exchange in colloidal systems, *J. Phys. Chem. B* 106 (45) (2002) 11746–11757, <https://doi.org/10.1021/jp020467r>.
- [15] J. Eastoe, M.J. Hollamby, L. Hudson, Recent advances in nanoparticle synthesis with reversed micelles, *Adv. Colloid Interface Sci.* 128–130 (2006) 5–15, <https://doi.org/10.1016/j.cis.2006.11.009>.
- [16] Y. Wang, R. Balaji, R.P. Quirk, W.L. Mattice, Detection of the rate of exchange of chains between micelles formed by diblock copolymers in aqueous solution, *Polym. Bull.* 28 (3) (1992) 333–338, <https://doi.org/10.1007/BF00294831>.
- [17] Y. Wang, C.M. Kausch, M. Chun, R.P. Quirk, W.L. Mattice, Exchange of chains between micelles of labeled polystyrene-block-poly(oxyethylene) as monitored by nonradiative singlet energy transfer, *Macromolecules* 28 (4) (1995) 904–911, <https://doi.org/10.1021/ma00108a016>.
- [18] B. Bednář, L. Karásek, J. Pokorný, Nonradiative energy transfer studies of block copolymers in selective solvents, *Polymer* 37 (23) (1996) 5261–5268, [https://doi.org/10.1016/0032-3861\(96\)00344-8](https://doi.org/10.1016/0032-3861(96)00344-8).
- [19] S. Creutz, J. van Stam, S. Antoun, F.C. De Schryver, R. Jérôme, Exchange of polymer molecules between block copolymer micelles studied by emission spectroscopy. A method for the quantification of unimer exchange rates, *Macromolecules* 30 (14) (1997) 4078–4083, <https://doi.org/10.1021/ma961922i>.
- [20] L. Willner, A. Poppe, J. Allgaier, M. Monkenbusch, D. Richter, Time-resolved SANS for the determination of unimer exchange kinetics in block copolymer micelles, *Europhys. Lett.* 55 (5) (2001) 667–673, <https://doi.org/10.1209/epl/i2001-00467-y>.
- [21] Y.-Y. Won, H.T. Davis, F.S. Bates, Molecular exchange in PEO–PB micelles in water, *Macromolecules* 36 (3) (2003) 953–955, <https://doi.org/10.1021/ma021439+>.
- [22] R. Lund, L. Willner, D. Richter, E.E. Dormidontova, Equilibrium chain exchange kinetics of diblock copolymer micelles: tuning and logarithmic relaxation, *Macromolecules* 39 (13) (2006) 4566–4575, <https://doi.org/10.1021/ma060328y>.
- [23] R. Lund, L. Willner, D. Richter, Kinetics of Block Copolymer Micelles Studied by Small-Angle Scattering Methods, Springer International Publishing, Cham, 2013, https://doi.org/10.1007/12_2012_204, pp. 51–158.
- [24] T. Narayanan, H. Wacklin, O. Konovalov, R. Lund, Recent applications of synchrotron radiation and neutrons in the study of soft matter, *Crystalllogr. Rev.* 23 (3) (2017) 160–226, <https://doi.org/10.1080/0889311X.2016.1277212>.
- [25] U. Tritschler, S. Pearce, J. Gwyther, G.R. Whittell, I. Manners, 50th anniversary perspective: Functional nanoparticles from the solution self-assembly of block copolymers, *Macromolecules* 50 (9) (2017) 3439–3463, <https://doi.org/10.1021/acs.macromol.6b02767>.
- [26] Z. Gao, S.K. Varshney, S. Wong, A. Eisenberg, Block copolymer “crew-cut” micelles in water, *Macromolecules* 27 (26) (1994) 7923–7927, <https://doi.org/10.1021/ma00104a058>.
- [27] L. Zhang, A. Eisenberg, Multiple morphologies of “crew-cut” aggregates of polystyrene-*b*-poly(acrylic acid) block copolymers, *Science* 268 (5218) (1995) 1728–1731, <https://doi.org/10.1126/science.268.5218.1728>.
- [28] L. Zhang, A. Eisenberg, Multiple morphologies and characteristics of “crew-cut” micelle-like aggregates of polystyrene-*b*-poly(acrylic acid) diblock copolymers in aqueous solutions, *J. Am. Chem. Soc.* 118 (13) (1996) 3168–3181, <https://doi.org/10.1021/ja953709s>.
- [29] S.L. Canning, G.N. Smith, S.P. Armes, A critical appraisal of RAFT-mediated polymerization-induced self-assembly, *Macromolecules* 49 (6) (2016) 1985–2001, <https://doi.org/10.1021/acs.macromol.5b02602>.
- [30] N.J. Warren, S.P. Armes, Polymerization-induced self-assembly of block copolymer nano-objects via RAFT aqueous dispersion polymerization, *J. Am. Chem. Soc.* 136 (29) (2014) 10174–10185, <https://doi.org/10.1021/ja502843f>.
- [31] M.J. Derry, L.A. Fielding, S.P. Armes, Polymerization-induced self-assembly of block copolymer nanoparticles via RAFT non-aqueous dispersion polymerization, *Prog. Polym. Sci.* 52 (2016) 1–18, <https://doi.org/10.1016/j.progpolymsci.2015.10.002>.
- [32] A.B. Lowe, RAFT alcoholic dispersion polymerization with polymerization-induced self-assembly, *Polymer* 106 (2016) 161–181.
- [33] M. Zong, K.J. Thurecht, S.M. Howdle, Dispersion polymerisation in supercritical CO₂ using macro-RAFT agents, *Chem. Commun.* (2008) 5942–5944, <https://doi.org/10.1039/B812827H>.
- [34] Q. Zhang, S. Zhu, Ionic liquids: versatile media for preparation of vesicles from polymerization-induced self-assembly, *ACS Macro Lett.* 4 (7) (2015) 755–758, <https://doi.org/10.1021/acsmacrolett.5b00360>.
- [35] K. Yamauchi, H. Hasegawa, T. Hashimoto, H. Tanaka, R. Motokawa, S. Koizumi, Direct observation of polymerization-reaction-induced molecular self-assembling process: In-situ and real-time SANS measurements during living anionic polymerization of polyisoprene-block-polystyrene, *Macromolecules* 39 (13) (2006) 4531–4539, <https://doi.org/10.1021/ma052696s>.
- [36] H. Tanaka, K. Yamauchi, H. Hasegawa, N. Miyamoto, S. Koizumi, T. Hashimoto, In situ and real-time small-angle neutron scattering studies of living anionic polymerization process and polymerization-induced self-assembly of block copolymers, *Physica B: Condens. Matter* 385–386 (2006) 742–744, <https://doi.org/10.1016/j.physb.2006.06.049>.
- [37] Y. Zhao, H. Tanaka, N. Miyamoto, S. Koizumi, T. Hashimoto, Combined SANS, SEC, NMR, and UV–vis studies of simultaneous living anionic copolymerization process: simultaneous elucidation of propagating living chains at three different length scales, *Macromolecules* 42 (5) (2009) 1739–1748, <https://doi.org/10.1021/ma8017519>.
- [38] Y. Zhao, N. Miyamoto, S. Koizumi, T. Hashimoto, Combined SANS, SEC, NMR, and UV–vis studies of simultaneous living anionic copolymerization process in a concentrated solution: elucidation of building-up processes of molecules and their self-assemblies, *Macromolecules* 43 (6) (2010) 2948–2959, <https://doi.org/10.1021/ma902542e>.
- [39] G.N. Smith, V.J. Cunningham, S.L. Canning, M.J. Derry, J.F.K. Cooper, A.L. Washington, S.P. Armes, Spin-echo small-angle neutron scattering (SESANS) studies of diblock copolymer nanoparticles, *Soft Matter* 15 (1) (2019) 17–21, <https://doi.org/10.1039/C8SM01425F>.
- [40] L.D. Blackman, K.E.B. Doncom, M.I. Gibson, R.K. O'Reilly, Comparison of photo- and thermally initiated polymerization-induced self-assembly: a lack of end group fidelity drives the formation of higher order morphologies, *Polym. Chem.* 8 (2017) 2860–2871, <https://doi.org/10.1039/C7PY00407A>.
- [41] E.J. Cornel, G.N. Smith, S.E. Rogers, J.E. Hallett, D.J. Gowney, T. Smith, P.S. O'Hara, S. van Meurs, O.O. Mykhaylyk, S.P. Armes, Time-resolved small-angle neutron scattering studies of the thermally-induced exchange of copolymer chains between spherical diblock copolymer nanoparticles prepared via polymerization-induced self-assembly, *Soft Matter* 16 (2020) 3657–3668, <https://doi.org/10.1039/c9sm02425e>.
- [42] L.A. Fielding, M.J. Derry, V. Ladmiraal, J. Rosselgong, A.M. Rodrigues, L.P.D. Ratcliffe, S. Sugihara, S.P. Armes, Raft dispersion polymerization in non-polar solvents: facile production of block copolymer spheres, worms and vesicles in n-alkanes, *Chem. Sci.* 4 (5) (2013) 2081–2087, <https://doi.org/10.1039/C3SC50305D>.
- [43] L.A. Fielding, J.A. Lane, M.J. Derry, O.O. Mykhaylyk, S.P. Armes, Thermo-responsive diblock copolymer worm gels in non-polar solvents, *J. Am. Chem. Soc.* 136 (15) (2014) 5790–5798, <https://doi.org/10.1021/ja501756h>.
- [44] M.J. Derry, L.A. Fielding, S.P. Armes, Industrially-relevant polymerization-induced self-assembly formulations in non-polar solvents: RAFT dispersion polymerization of benzyl methacrylate, *Polym. Chem.* 6 (16) (2015) 3054–3062, <https://doi.org/10.1039/C5PY00157A>.
- [45] K.L. Thompson, L.A. Fielding, O.O. Mykhaylyk, J.A. Lane, M.J. Derry, S.P. Armes, Vermiciform thermo-responsive pickering emulsifiers, *Chem. Sci.* 6 (2015) 4207–4214, <https://doi.org/10.1039/C5SC00598A>.
- [46] CRC, Viscosity of liquids, in: *CRC Handbook of Chemistry and Physics*, 95th ed., CRC Press, 2014–2015 (Internet Version).
- [47] V.F. Sears, Neutron scattering lengths and cross sections, *Neutron News* 3 (3) (1992) 26–37, <https://doi.org/10.1080/10448639208218770>.
- [48] C.D. Dewhurst, I. Grillo, D. Honecker, M. Bonnaud, M. Jacques, C. Amrouni, A. Perillo-Marcone, G. Manzin, R. Cubitt, The small-angle neutron scattering instrument D33 at the Institut Laue-Langevin, *J. Appl. Cryst.* 49 (1) (2016) 1–14, <https://doi.org/10.1107/S1600576715021792>.
- [49] I. Grillo, Small-Angle Neutron Scattering and Applications in Soft Condensed Matter, Springer, Netherlands, Dordrecht, 2008, pp. 723–782, https://doi.org/10.1007/978-1-4020-4465-6_13.
- [50] M. Doucet, et al., Sasview version 5.0.2, Zenodo.doi:10.5281/zenodo.3752443.
- [51] I. Reynolds, Poly (lauryl methacrylate): spread monolayers and bulk configuration, Ph.D. thesis, University of Durham (1995). URL <http://theses.dur.ac.uk/5448/>.
- [52] J.S. Pedersen, M.C. Gerstenberg, Scattering form factor of block copolymer micelles, *Macromolecules* 29 (4) (1996) 1363–1365, <https://doi.org/10.1021/ma9512115>.
- [53] J.S. Pedersen, Form factors of block copolymer micelles with spherical, ellipsoidal and cylindrical cores, *J. Appl. Cryst.* 33 (3 Part 1) (2000) 637–640, <https://doi.org/10.1107/S0021889899012248>.
- [54] R. Heenan, Sasview 5.0.2 documentation polymer_micelle. URL: http://www.sasview.org/docs/user/models/polymer_micelle.html.
- [55] Lord Rayleigh, The incidence of light upon a transparent sphere of dimensions comparable with the wave-length, *Proc. R. Soc. London A* 84 (567) (1910) 25–46, <https://doi.org/10.1098/rspa.1910.0054>.

- [56] A. Guinier, G. Fournet, *Small-Angle Scattering of X-Rays*, John Wiley & Sons, New York, 1955.
- [57] P. Debye, Molecular-weight determination by light scattering, *J. Phys. Chem.* 51 (1) (1947) 18–32, <https://doi.org/10.1021/j150451a002>.
- [58] J. Trehwella, A.P. Duff, D. Durand, F. Gabel, J.M. Guss, W.A. Hendrickson, G.L. Hura, D.A. Jacques, N.M. Kirby, A.H. Kwan, J. Pérez, L. Pollack, T.M. Ryan, A. Sali, D. Schneidman-Duhovny, T. Schwede, D.I. Svergun, M. Sugiyama, J.A. Tainer, P. Vachette, J. Westbrook, A.E. Whitten, 2017 publication guidelines for structural modelling of small-angle scattering data from biomolecules in solution: an update, *Acta Crystallogr., Sect. D: Struct. Biol.* 73(9) (2017) 710–728. doi:10.1107/S2059798317011597.
- [59] L.S. Bartell, On the length of the carbon–carbon single bond, *J. Am. Chem. Soc.* 81 (14) (1959) 3497–3498, <https://doi.org/10.1021/ja01523a002>.
- [60] F.H. Allen, O. Kennard, D.G. Watson, L. Brammer, A.G. Orpen, R. Taylor, Tables of bond lengths determined by X-ray and neutron diffraction. Part 1. Bond lengths in organic compounds, *J. Chem. Soc., Perkin Trans. 2*(12) (1987), S1–S19, <https://doi.org/10.1039/P29870000051>.
- [61] D.R. Lide, Structure of free molecules in the gas phase. Part 2. Molecules containing carbon, in: W.M. Haynes (Ed.), *CRC Handbook of Chemistry and Physics*, 97th ed., CRC Press, Boca Raton, FL, 2016–2017, pp. 9–31–9–55.
- [62] S.M. Aharoni, On entanglements of flexible and rodlike polymers, *Macromolecules* 16 (11) (1983) 1722–1728, <https://doi.org/10.1021/ma00245a008>.
- [63] S.M. Aharoni, Correlations between chain parameters and the plateau modulus of polymers, *Macromolecules* 19 (2) (1986) 426–434, <https://doi.org/10.1021/ma00156a033>.
- [64] R.G. Kirste, R.C. Oberthür, *Synthetic polymers in solution*, in: O. Glatter, O. Kratky (Eds.), *Small Angle X-ray Scattering*, 12, Academic Press, London, 1982, pp. 387–432.
- [65] G.N. Smith, L.L.E. Mears, S.E. Rogers, S.P. Armes, Synthesis and electrokinetics of cationic spherical nanoparticles in salt-free non-polar media, *Chem. Sci.* 9 (4) (2018) 922–934, <https://doi.org/10.1039/C7SC03334F>.
- [66] G.N. Smith, Proton transfer in nonpolar solvents: an approach to generate electrolytes in aprotic media, *Phys. Chem. Chem. Phys.* 20 (2018) 18919–18923, <https://doi.org/10.1039/C8CP02349B>.
- [67] S. Harrisson, The downside of dispersity: why the standard deviation is a better measure of dispersion in precision polymerization, *Polym. Chem.* 9 (12) (2018) 1366–1370, <https://doi.org/10.1039/C8PY00138C>.
- [68] A. Lapp, C. Picot, H. Benoit, Determination of the Flory interaction parameters in miscible polymer blends by measurement of the apparent radius of gyration, *Macromolecules* 18 (12) (1985) 2437–2441, <https://doi.org/10.1021/ma00154a017>.
- [69] S. King, Sasview Marketplace/ Binary Blend. <http://marketplace.sasview.org/models/124/>.
- [70] F.D. Blum, E.N. Young, G. Smith, O.C. Sitton, Thermal analysis of adsorbed poly (methyl methacrylate) on silica, *Langmuir* 22 (10) (2006) 4741–4744, <https://doi.org/10.1021/la053098+>.
- [71] Z. Liu, G. Zhang, W. Lu, Y. Huang, J. Zhang, T. Chen, Uv light-initiated RAFT polymerization induced self-assembly, *Polym. Chem.* 6 (2015) 6129–6132, <https://doi.org/10.1039/C5PY00907C>.
- [72] J. Tan, H. Sun, M. Yu, B.S. Sumerlin, L. Zhang, Photo-PISA: Shedding light on polymerization-induced self-assembly, *ACS Macro Lett.* 4 (11) (2015) 1249–1253, <https://doi.org/10.1021/acsmacrolett.5b00748>.
- [73] T.G. McKenzie, Q. Fu, M. Uchiyama, K. Satoh, J. Xu, C. Boyer, M. Kamigaito, G.G. Qiao, Beyond traditional RAFT: alternative activation of thiocarbonylthio compounds for controlled polymerization, *Adv. Sci.* 3 (9) (2016) 1500394, <https://doi.org/10.1002/advs.201500394>.
- [74] J. Yeow, C. Boyer, Photoinitiated polymerization-induced self-assembly (Photo-PISA): new insights and opportunities, *Adv. Sci.* 4 (7) (2017) 1700137, <https://doi.org/10.1002/advs.201700137>.
- [75] G. N. Smith, J. Eastoe, I. Grillo, J. Hallett, J. Peach, J. Pegg, Surfactant-induced charging of polydimethylsiloxane-poly(methyl methacrylate) latexes in nonpolar solvents, *Institut Laue-Langevin (ILL)* doi:10.5291/ILL-DATA.9-12-478 (2016).